Supporting Information

Efficient separation of CO$_2$ from CH$_4$ and N$_2$ in an ultra-stable microporous metal-organic framework

Chaohui He*, Peng Zhang, Sai Ma, Yujuan Zhang, Tuoping Hu*

Department of Chemistry, College of Chemistry and Chemical Engineering, North University of China, Taiyuan, 030051, Shanxi, P. R. China

Isosteric heat of adsorption

The isosteric heats of adsorption (Q_{st}) were calculated from single-component adsorption isotherms of CO_2 measured at 273, 298 and 313 K. The isotherms were fit to a viral Eq.

$$\ln P = \ln N + \frac{1}{T}\sum_{i=o}^{m} a_i Ni + \sum_{j=o}^{n} b_j Nj$$

Where N is the amount of gas adsorbed at pressure P, a_i and b_j are virial coefficients, m and n are the numbers of coefficients require to adequately describe the isotherm. Using the fitting parameters obtained from the above equation, Q_{st} can be calculated using the following Eq.

$$Q_{st} = - R\sum_{i=o}^{m} a_i N^i$$

R is the universal gas constant.

Ideal adsorbed solution theory (IAST) calculations

The single-component adsorption isotherms of CO_2, CH_4 and N_2 on Y-bptc obtained at 298 K were fitted using the dual site Langmuir model.

$$q = q_{A,sat}\frac{b_A p}{1 + b_A p} + q_{B,sat}\frac{b_B p}{1 + b_B p}$$

where q represents the adsorbed capacity per mass of adsorbent (mol/kg), $q_{A,sat}$ and $q_{B,sat}$ are the saturation uptake capacities at site A and site B, respectively, b_A and b_B represent the constant at adsorption site A and site B, respectively, P represents the total pressure of the gas at the equilibrium (kPa).

The adsorption selectivity defined as follows:

$$S_{ads} = \frac{q_A/q_B}{y_A/y_B}$$

where q_A and q_B represent the component molar loading within the MOFs and y_A and

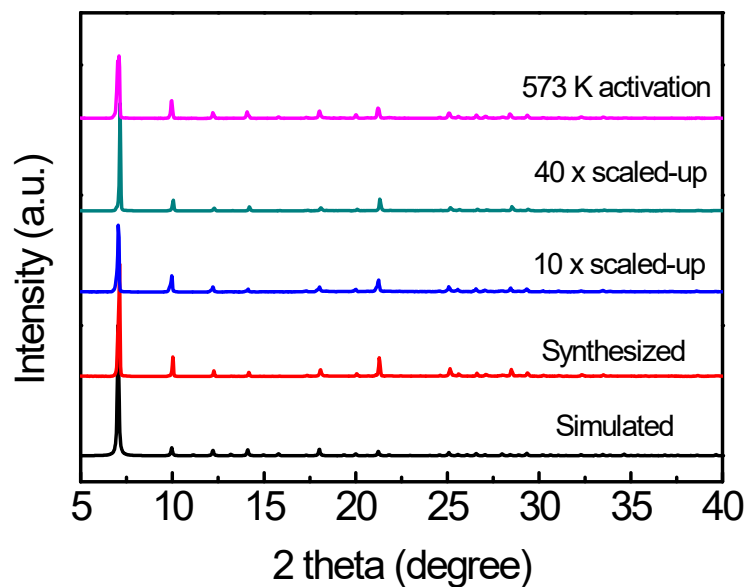y_B are the corresponding mole fraction used in the feed gas mixture.

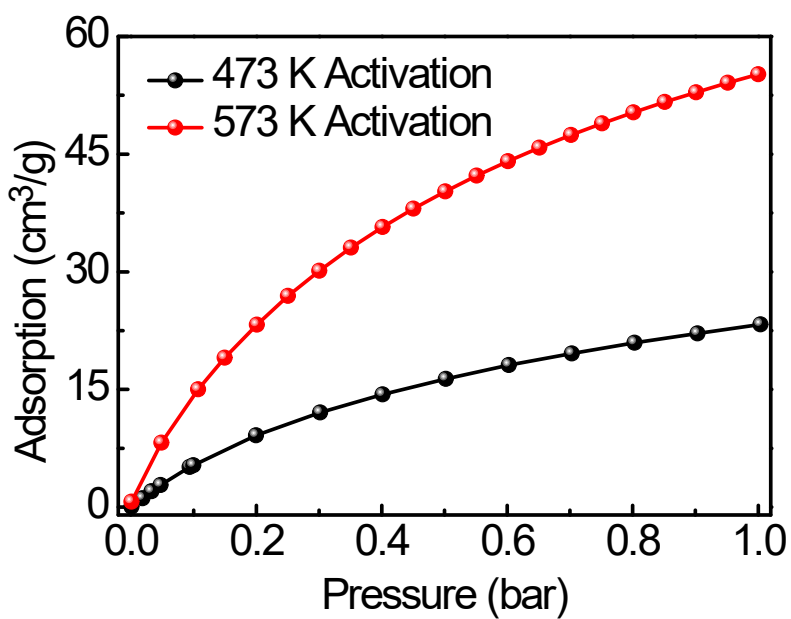**Fig. S1.** PXRD patterns recorded for Y-bptc.

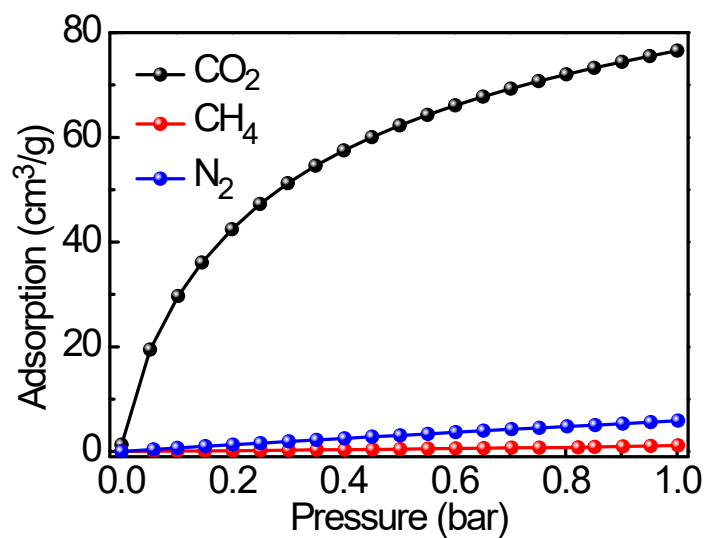**Fig. S2.** The single-adsorption isotherms of Y-bptc for CO_2 at different activation temperatures.

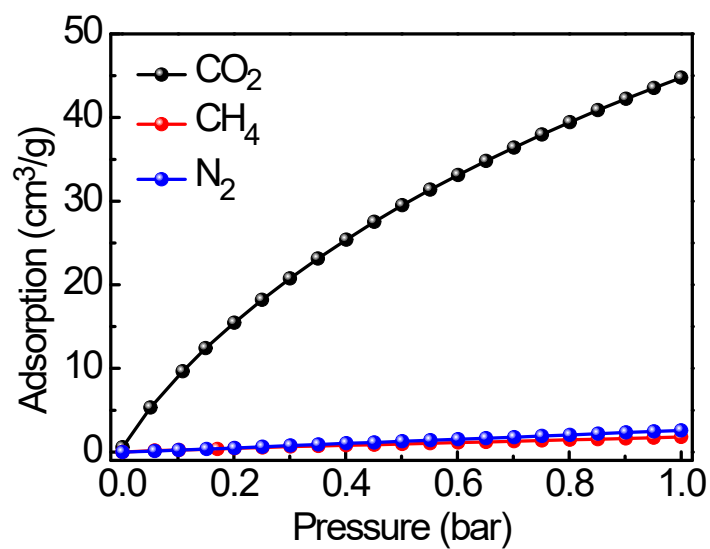**Fig. S3.** The single-adsorption isotherms of Y-bptc for CO_2, CH_4 and N_2 at 273 K.

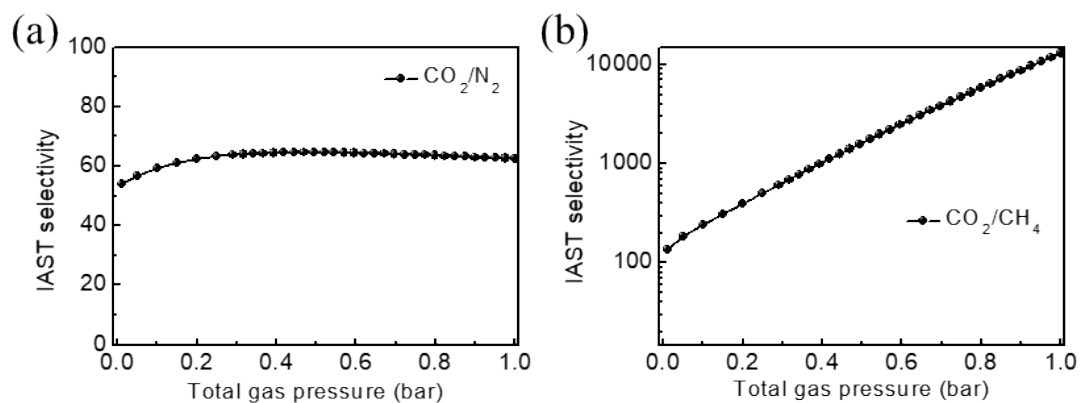**Fig. S4.** The single-adsorption isotherms of Y-bptc for CO_2, CH_4 and N_2 at 313 K.

Fig. S5. The adsorption selectivity of (a) CO_2/N_2 (0.15/0.85) and (b) CO_2/CH_4 (1/1) for Y-bptc at 298 K.

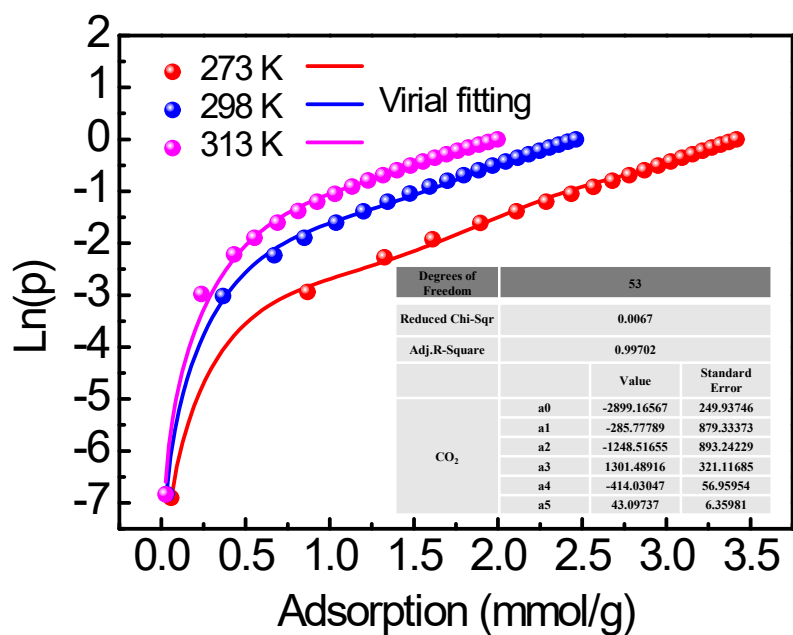|		Value	Standard Error
Degrees of Freedom		53	
Reduced Chi-Sqr		0.0067	
Adj.R-Square		0.99702	
CO_2	a0	-2899.16567	249.93746
	a1	-285.77789	879.33373
	a2	-1248.51655	893.24229
	a3	1301.48916	321.11685
	a4	-414.03047	56.95954
	a5	43.09737	6.35981

Fig. S6. CO_2 fitting isotherms of Y-bptc through virial equation.
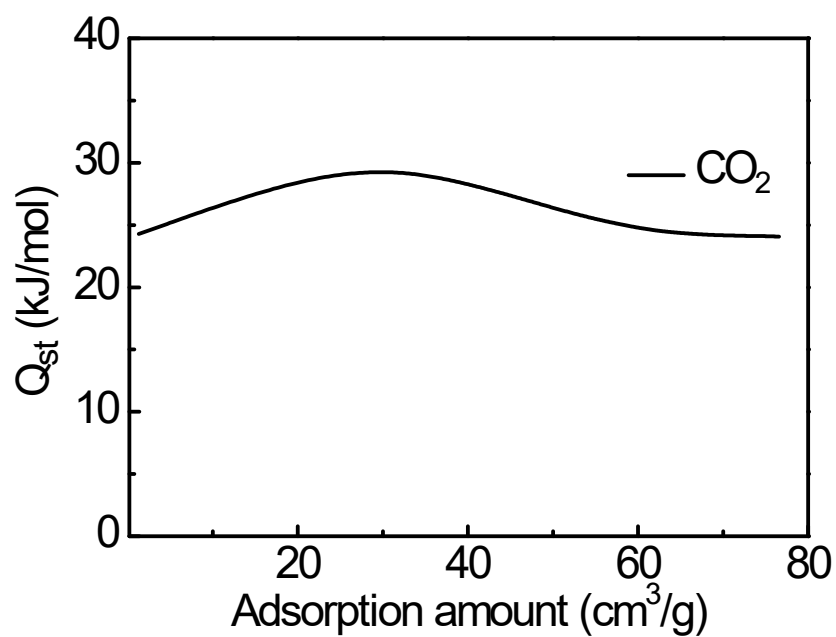
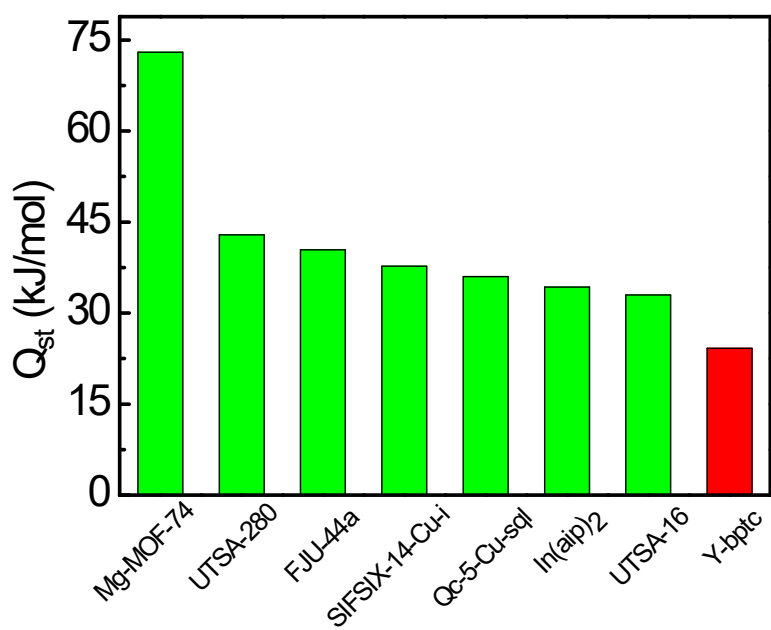**Fig. S7.** The adsorption heat of Y-bptc for CO_2.

Fig. S8. The comparison of adsorption heat of reported CO_2 adsorbents.
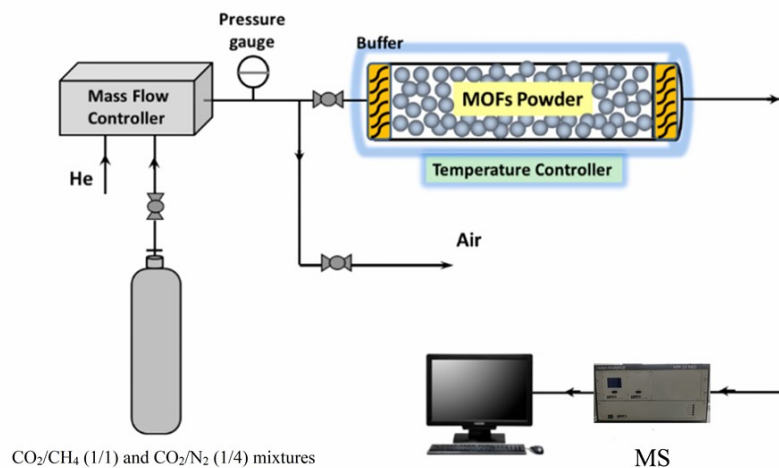
Fig. S9. The breakthrough experimental set-up schematic under dry conditions.
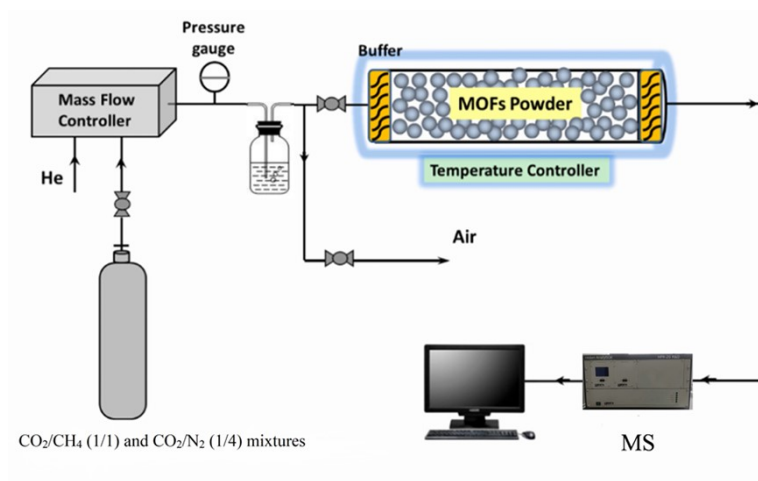

Fig. S10. The breakthrough experimental set-up schematic under wet conditions.
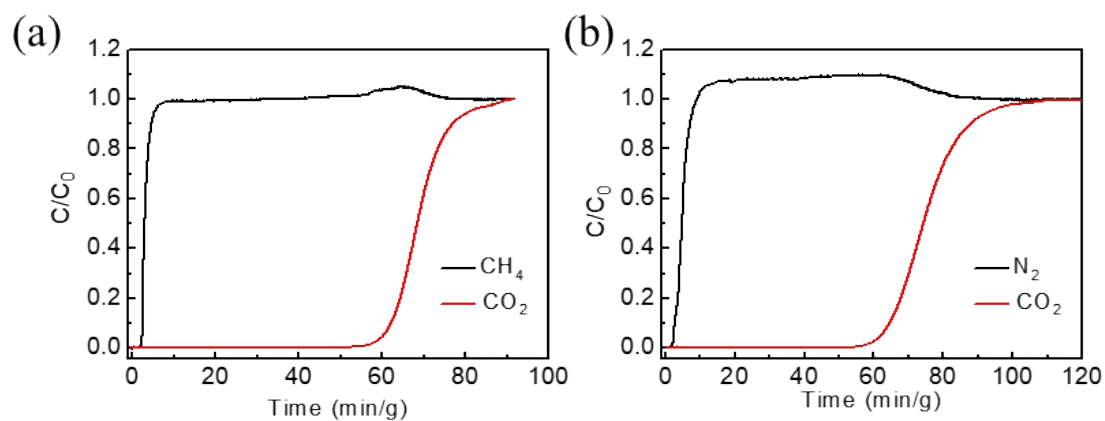

Fig. S11. Breakthrough experiments using Y-bptc for wet CO_2/CH_4 (1/1) and CO_2/N_2

(1/4) mixtures at 298 K.

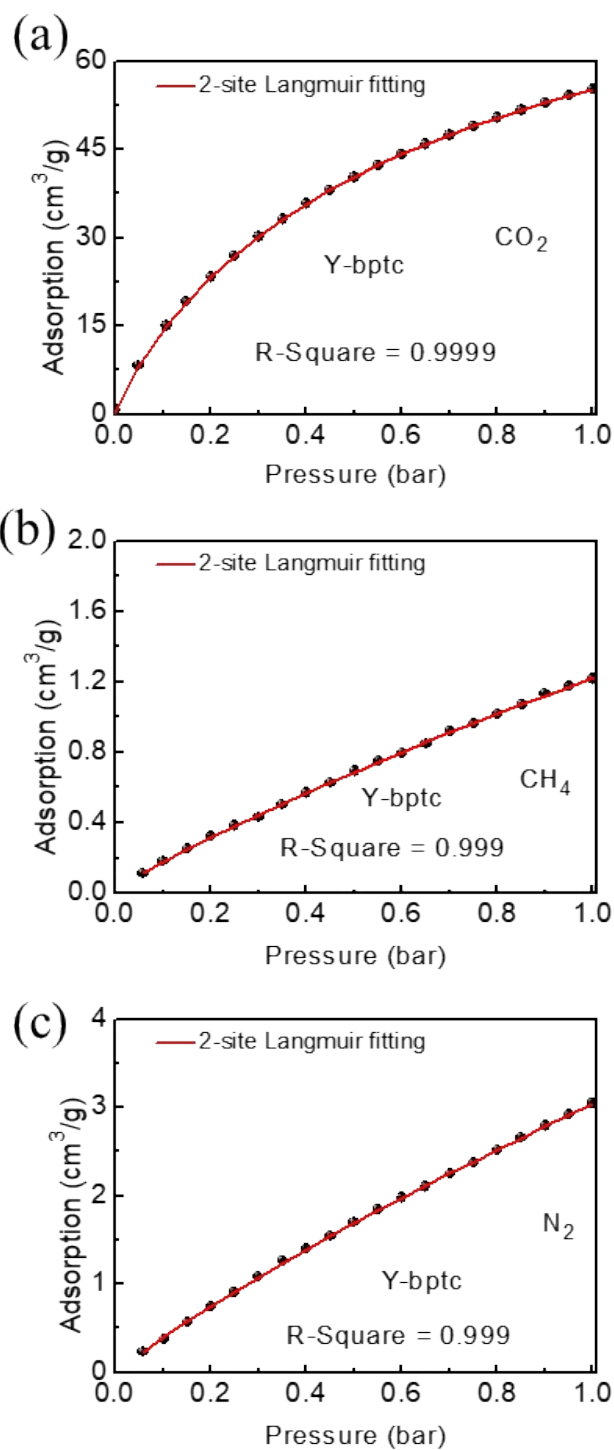**Fig. S12.** CO_2, CH_4 and N_2 adsorption isotherms at 298 K in Y-bptc with dual-site Langmuir model fits.
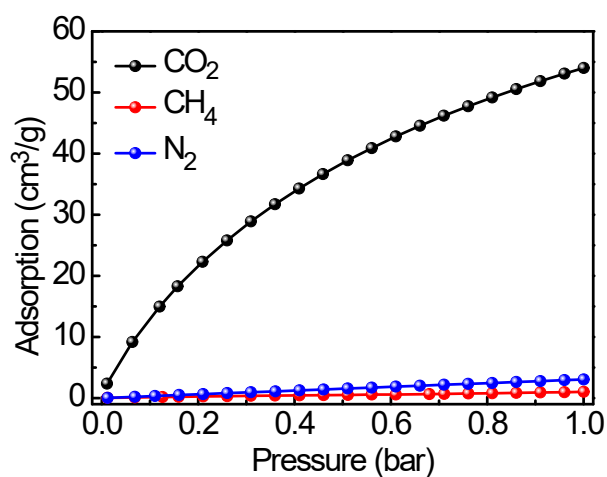
Fig. S13. The equilibrium adsorption isotherms of Y-bptc (~250 mg) for CO_2, CH_4, and
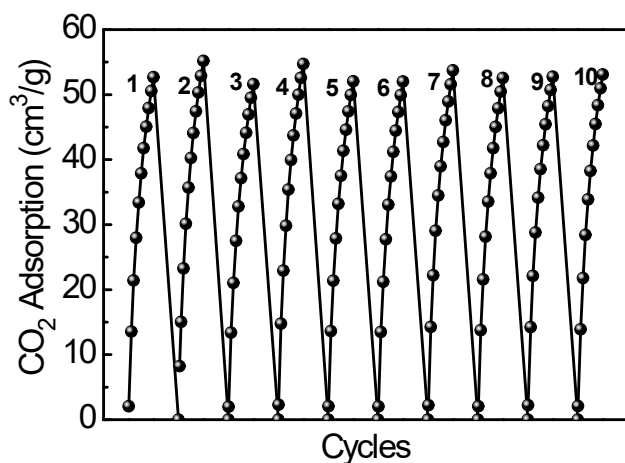
N_2 at 298 K.

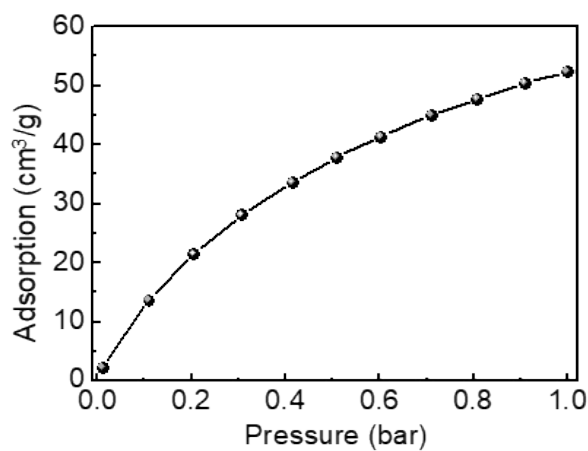**Fig. S14.** Adsorption-desorption cycles for CO_2 in Y-bptc at 1 bar and 298 K.

Fig. S15. The equilibrium adsorption isotherms of Y-bptc for CO_2 after activation at

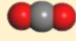573 K for 12 h.

Table S1 Physicochemical properties of CO_2, CH_4 and N_2

	Structure	Molecular size (Å^3)	Kinetic diameter (Å)	Boiling point (K)	Polarizability ($\times 10^{-25}$/cm^3)	Quadrupole moment ($\times 10^{26}$/esu cm^2)
CO_2		$3.18 \times 3.33 \times 5.36$	3.3	194.7	29.11	-4.30
CH_4		$3.7 \times 3.7 \times 3.7$	3.758	111.66	25.93	0
N_2		$3.6 \times 3.6 \times 3.6$	3.64	77.35	17.403	1.52

Table S2 Summary of the equilibrium uptakes, CO_2/CH_4 and CO_2/N_2 uptake ratio in some reported MOFs.

Adsorbents	CO_2 uptake (cm^3/g)	CH_4 uptake (cm^3/g)	N_2 uptake (cm^3/g)	CO_2/CH_4 uptake ratio	CO_2/N_2 uptake ratio	Reference
Y-bptc	55.1	1.21	3.04	45.5	18.1	This work
In(aip)$_2$	28.1	0.4	0.2	70.2	140.5	[1]
Qc-5-Cu-sql	48.4	1.3	0.3	37.2	161.3	[2]
SIFSIX-3-Zn	56.2	9	3.4	6.2	16.5	[3]
CALF-20	60.5	-	5.2	-	11.6	[4]
Mg-MOF-74	192.9	23.52	-	8.2	-	[5]
ZIF-8	18.1	6.3	2.2	2.87	8.22	[6]
UTSA-16	76.2	10.3	1.4	7.39	54.4	[7]
NJUBai35	72.8	20.2	4	3.6	18.2	[8]
FJU-44a	53.2	11.3	2.7	4.7	19.7	[9]
Cu-Fpymo	39.2	0.89	0.33	44	118	[10]
UTSA-280	67.3	4	6	16.8	11.2	[11]
SIFSIX-14-Cu-i	106	0.92	-	115.2	-	[12]

NOTT-400	109.7	17.92	-	6.1	-	[13]
NOTT-401	64.9	20.1	-	3.2	-	[13]

Table S3 Dual-Langmuir fitting parameters for CO_2, CH_4 and N_2 in Y-bptc at 298 K.

	Site A		Site B	
	$q_{A,sat}$	b_A	$q_{B,sat}$	b_B
	$cm^3\ g^{-1}$	bar^{-1}	$cm^3\ g^{-1}$	bar^{-1}
CO_2	7.39	0.06	84.56	0.75
CH_4	0.06	0.04	8.29	6.14
N_2	4.40	2.20	2.11	1.04

Table S4 The element analysis of Y-bptc after activation at different temperatures.

	"N"content (%)	$[H_2N(CH_3)_2]^+$ (%)
473 K activation	3.42	11.23
573 K activation	1.79	5.88

The quantity of ammonium ions was calculated by measuring the "N" content through Element Analysis.

References

1. Y.-M. Gu, H.-F. Qi, S. Qadir, T.-J. Sun, R. Wei, S.-S. Zhao, X.-W. Liu, Z. Lai and S.-D. Wang, *Chem. Eng. J.*, 2022, **449**, 137768.

2. K.-J. Chen, D. G. Madden, T. Pham, K. A. Forrest, A. Kumar, Q.-Y. Yang, W. Xue, B. Space, J. J. Perry IV, J.-P. Zhang, X.-M. Chen and M. J. Zaworotko, *Angew. Chem. Int. Ed.*, 2016, **55**, 10268-10272.

3. P. Nugent, Y. Belmabkhout, S. D. Burd, A. J. Cairns, R. Luebke, K. Forrest, T. Pham, S. Ma, B. Space, L. Wojtas, M. Eddaoudi and M. J. Zaworotko, *Nature*, 2013, **495**, 80-84.

4. J.-B. Lin, T. T. T. Nguyen, R. Vaidhyanathan, J. Burner, J. M. Taylor, H. Durekova, F. Akhtar, R. K. Mah, O. Ghaffari-Nik, S. Marx, N. Fylstra, S. S. Iremonger, K. W. Dawson, P. Sarkar, P. Hovington, A. Rajendran, T. K. Woo and G. K. H. Shimizu, *Science*, 2021, **374**, 1464-1469.

5. Z. Bao, L. Yu, Q. Ren, X. Lu and S. Deng, *J. Colloid Interface Sci.*, 2011, **353**, 549-556.

6. J. McEwen, J.-D. Hayman and A. Ozgur Yazaydin, *Chem. Phys.*, 2013, **412**, 72-76.

7. S. Xiang, Y. He, Z. Zhang, H. Wu, W. Zhou, R. Krishna and B. Chen, *Nat. Commun.*, 2012, **3**, 954.

8. J. Jiang, Z. Lu, M. Zhang, J. Duan, W. Zhang, Y. Pan and J. Bai, *J. Am. Chem. Soc.*, 2018, **140**, 17825-17829.

9. Y. Ye, H. Zhang, L. Chen, S. Chen, Q. Lin, F. Wei, Z. Zhang and S. Xiang,

Inorg. Chem., 2019, **58**, 7754-7759.

10. Y. Shi, Y. Xie, H. Cui, Z. A. Alothman, O. Alduhaish, R.-B. Lin and B. Chen, *Chem. Eng. J.*, 2022, **446**, 137101.

11. R.-B. Lin, L. Li, A. Alsalme and B. Chen, *Small Structures*, 2020, **1**, 2000022.

12. M. Jiang, B. Li, X. Cui, Q. Yang, Z. Bao, Y. Yang, H. Wu, W. Zhou, B. Chen and H. Xing, *ACS. Appl. Mater. Interfaces.*, 2018, **10**, 16628-16635.

13. I. A. Ibarra, A. Mace, S. Yang, J. Sun, S. Lee, J.-S. Chang, A. Laaksonen, M. Schröder and X. Zou, Inorg. Chem., 2016, 55, 7219-7228.